Automatic segmentation for plan-of-the-day selection in CBCT-guided adaptive radiation therapy of cervical cancer

Chen Zhang, Caroline Lafond, Anaïs Barateau, Julie Leseur, Bastien Rigaud, Diane-Barbara Chan Sock Line, Guanyu Yang, Huazhong Shu, Jean-Louis Dillenseger, Renaud de Crevoisier, et al.

▶ **To cite this version:**

Chen Zhang, Caroline Lafond, Anaïs Barateau, Julie Leseur, Bastien Rigaud, et al.. Automatic segmentation for plan-of-the-day selection in CBCT-guided adaptive radiation therapy of cervical cancer. Physics in Medicine and Biology, 2022, 67 (24), pp.245020. 10.1088/1361-6560/aca5e5 . hal-03882318

HAL Id: hal-03882318
https://hal.science/hal-03882318

Submitted on 2 Dec 2022

HAL is a multi-disciplinary open access archive for the deposit and dissemination of scientific research documents, whether they are published or not. The documents may come from teaching and research institutions in France or abroad, or from public or private research centers.

L'archive ouverte pluridisciplinaire **HAL**, est destinée au dépôt et à la diffusion de documents scientifiques de niveau recherche, publiés ou non, émanant des établissements d'enseignement et de recherche français ou étrangers, des laboratoires publics ou privés.

IOP Publishing Journal Title
Journal **XX** (XXXX) XXXXXX https://doi.org/XXXX/XXXX

Automatic segmentation for plan-of-the-day selection in CBCT-guided adaptive radiation therapy of cervical cancer

Chen Zhang[1,2,3], Caroline Lafond[2], Anaïs Barateau[2], Julie Leseur[5], Bastien Rigaud[2], Diane Barbara Chan Sock Line[2], Guanyu Yang[1,2,4], Huazhong Shu[1,3,4,*], Jean-Louis Dillenseger[2,4], Renaud de Crevoisier[2] and Antoine Simon [2,4]

[1] Laboratory of Image Science and Technology, School of Computer Science and Engineering, Southeast University, Nanjing, China
[2] Univ Rennes, CLCC Eugène Marquis, Inserm, LTSI – UMR 1099, F-35000 Rennes, France
[3] Jiangsu Provincial Joint International Research Laboratory of Medical Information Processing, School of Computer Science and Engineering, Southeast University, Nanjing, China
[4] Centre de Recherche en Information Biomédical Sino-français (CRIBs), France
[5] CLCC Eugène Marquis, F-35000 Rennes, France
[*] Corresponding author

E-mail : shu.list@seu.edu.cn

Objective: Plan-of-the-day (PoD) adaptive radiation therapy (ART) is based on a library of treatment plans, among which, at each treatment fraction, the PoD is selected using daily images. However, this strategy is limited by PoD selection uncertainties. This work aimed to propose and evaluate a workflow to automatically and quantitatively identify the PoD for cervix cancer ART based on daily CBCT images.

Approach: The quantification was based on the segmentation of the main structures of interest in the CBCT images (clinical target volume [CTV], rectum, bladder, and bowel bag) using a deep learning model. Then, the PoD was selected from the treatment plan library according to the geometrical coverage of the CTV. For the evaluation, the resulting PoD was compared to the one obtained considering reference CBCT delineations.

Main results: In experiments on a database of 23 patients with 272 CBCT images, the proposed method obtained an agreement between the reference PoD and the automatically identified PoD for 91.5% of treatment fractions (99.6% when considering a 5% margin on CTV coverage).

 © xxxx IOP Publishing Ltd

IOP Publishing Journal Title
Journal **XX** (XXXX) XXXXXX https://doi.org/XXXX/XXXX

Significance: The proposed automatic workflow automatically selected PoD for ART using deep-learning methods. The results showed the ability of the proposed process to identify the optimal PoD in a treatment plan library.

1. Introduction

The standard treatment for locally advanced cervical cancer (LACC) is external beam radiotherapy (EBRT) with chemotherapy, followed by brachytherapy. Although Intensity-Modulated Radiation Therapy (IMRT) is used to reduce normal tissue toxicity (Naik *et al* 2016, Gandhi *et al* 2013), it is limited by large and complex intrapelvic anatomical variations occurring between the treatment fractions (Buchali *et al* 1999, Han *et al* 2006). The position and shape of the clinical target volume (CTV, including the cervix, uterus, upper-vagina, and parametrium) are highly dependent on bladder and rectum filling, and on tumor regression during treatment (Jadon *et al* 2014, Chan *et al* 2008, Beadle *et al* 2009). In the context of adaptive radiation therapy (ART), plan-of-the-day (PoD) strategies have been proposed based on the generation of a treatment plan library, including several treatment plans optimized according to multiple planning CTs (pCT) acquired with various bladder fillings (Bondar *et al* 2012, Heijkoop *et al* 2014, van de Schoot *et al* 2017). At each treatment fraction, the treatment plan is then selected among those of the library ("plan-of-the-day") based on an in-room image (e.g., CBCT image, see Figure 1). Although this strategy appears to be adequate to compensate for uterine motions (Heijkoop *et al* 2014, van de Schoot *et al* 2017, Gobeli *et al* 2015), it remains complex in a clinical workflow.

Different factors limit the rapid advancement of PoD ART. The PoD selection is actually a difficult process, mainly due to the poor contrast of CBCT images and large anatomical deformations. Thus, the expert needs to visualize the full 3D volume to assess the coverage of the whole target by the available treatment plans. The PoD selection is therefore a time-consuming process which is submitted to interobserver variability, as demonstrated in (Gobeli *et al* 2018) where 26 operators manually selected PoD on 24 CBCT images. This study showed a high inter-observer variablility since the optimal PoD was chosen on average by 60% of users.

In order to automatize PoD selection, the automatic segmentation of CBCT images has been proposed to measure, at each treatment fraction, the ability of the treatment plans to treat the target (Bondar *et al* 2013). Langerak et al. (Langerak *et al* 2014) proposed to use a multi-atlas-based segmentation method. On a total of 224 CBCT, the CBCT images corresponding to low confidence levels were firstly removed, resulting to 187 images on which the Dice values were 0.85, 0.81, and 0.80 for the uterus, bladder, and rectum, respectively. However, the CBCT image quality is limited by noise, artifacts, and low soft-tissue contrast, making automatic segmentation very challenging. Recently, with the widespread use of deep learning (DL) in medical imaging, Beekman et al. (Beekman *et al* 2022) compared different DL models, performing either direct segmentation or a segmentation prior deformation by diffeomorphic image registration. The deformation-based model performed the best on the CBCT test set, with a median Dice score of 0.80.

In the context of PoD-based ART for LACC, this work aimed to propose a strategy to automatically select the optimal treatment plan. It relies on a deep learning-based segmentation of the CBCT images, enabling the selection of the optimal treatment plan regarding the CTV coverage based on a geometrical criterion. This strategy was simulated and compared to a reference obtained from expert manual delineations.

 © xxxx IOP Publishing Ltd

IOP Publishing Journal Title
Journal **XX** (XXXX) XXXXXX https://doi.org/XXXX/XXXX

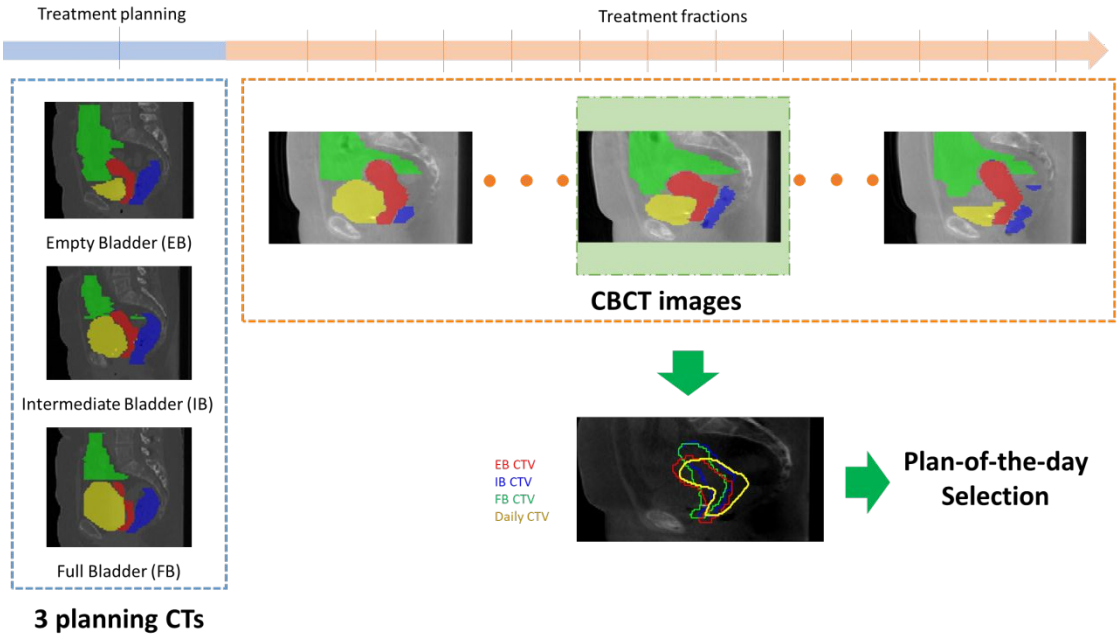

Figure 1. Flowchart of plan-of-the-day ART for cervical cancer. The process includes three steps (1) Planning: acquisition of multiple planning CT scans with variable bladder volumes. (2) Acquisition of the CBCT image of the day. (3) Selection of the most appropriate treatment plan to maximize the target coverage.

The CTV, bowel bag, bladder, and rectum are represented as red, green, yellow, and blue-filled contours. For plan-of-the-day selection, empty bladder (EB), intermediate bladder (IB), full bladder (FB), and daily CTV are represented on the daily CBCT as red, blue, green, and yellow contours, respectively.

2. Materials and methods

Figure 2 describes the flowchart of the study. Based on three planning CT scans, corresponding to empty bladder, intermediate bladder and full bladder, and on daily CBCT scans, it contains two parts applied to each daily CBCT image: (1) segmentation of the CBCT image using a deep learning network; (2) selection of the most appropriate PoD among the available planning CTs (pCTs). For this second step, the three pCTs in the planning library were registered to the daily CBCT image to simulate patient repositioning. Then, the coverage of the segmented daily CTV by the CTVs of pCTs was computed. Finally, the best treatment plan was selected as the one corresponding to the highest daily CTV coverage.

 © xxxx IOP Publishing Ltd

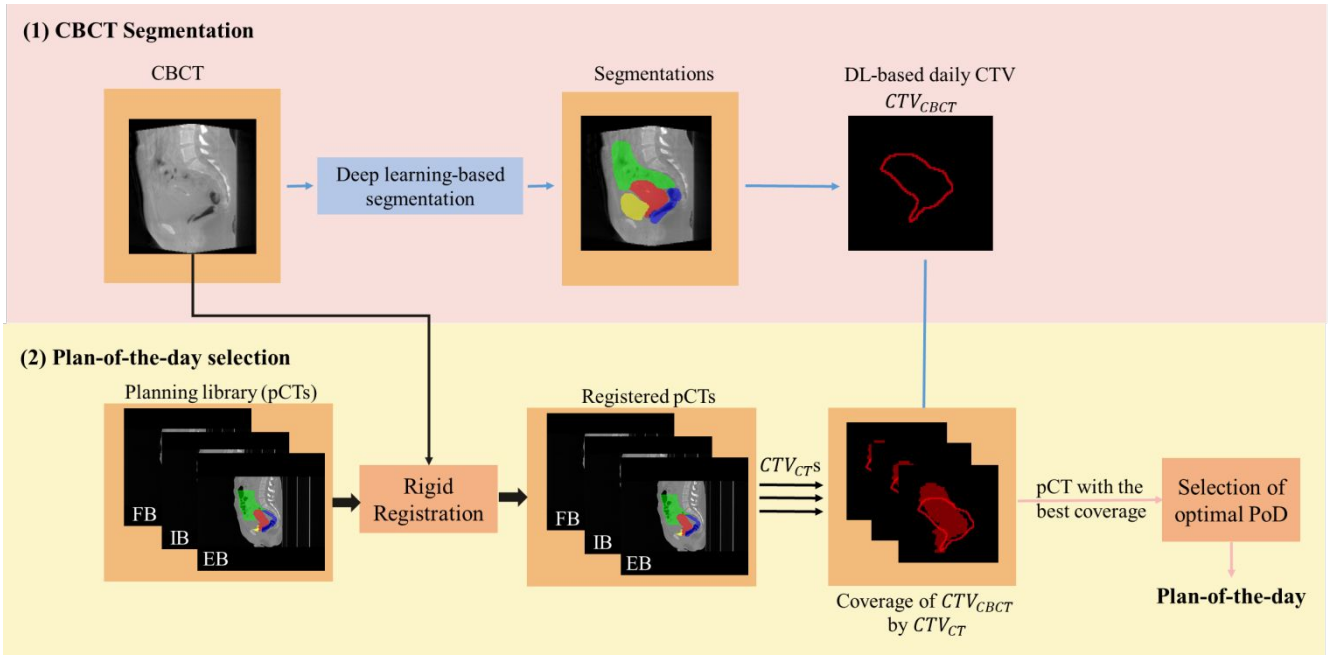

Figure 2. Flowchart of the study. The steps are: (1) CBCT segmentation using deep learning and (2) plan-of-the-day (PoD) selection using clinical target volume (CTV) contours. The PoD selection relies on: (a) Bone-based rigid registration of the planning CTs (pCTs) with the daily CBCT to simulate patient repositioning; (b) computation of the coverage between the daily CTV ($\boldsymbol{CTV_{CBCT}}$) and CTV of the pCTs ($\boldsymbol{CTV_{EB}}$, $\boldsymbol{CTV_{IB}}$, $\boldsymbol{CTV_{FB}}$); (c) selection of the best treatment plan based on target coverage: the pCT corresponding to the highest coverage was selected. (EB: empty bladder; IB: intermediate bladder; FB: Full bladder; cov: coverage value).

2.1 Data acquisition and experimental settings

In this study, we collected 272 CBCT scans and 63 CT scans from 23 patients. All patients were treated with a combination of external beam radiation therapy (EBRT) and pulse-dose-rate brachytherapy (PDR-BT). EBRT delivered a total dose of 45 Gy to the pelvis (supine position), at 1.8 Gy per fraction, using IMRT along with concomitant weekly cisplatin (40 mg/ m^2). PDR-BT was delivered following the GEC-ESTRO recommendations. All patients provided signed informed consent.

Each patient underwent two or three planning CTs with different bladder volumes: empty bladder (EB), intermediate bladder (IB), and full bladder (FB). One hour before the first IB CT, the patient had to drink 250 mL of water. Then another 500 mL of water should be consumed to obtain FB CT after 20 minutes. For EB CT, the patient emptied her bladder. All CTs were scanned (Big Bore, Philips) with voxel spacing ranging from 0.87×0.87×3.00 mm^3 to 1.21×1.21×3.00 mm^3. The dimensions range of CT volumes was from 75×512×512 to 168×512×512.

During the radiation therapy treatment, 5 to 16 CBCT images were acquired (XVI mounted on a Synergy linac, Elekta) for each patient with voxel spacing of 1.00×1.00×2.00 mm^3 and dimensions of 132×410×410.

All images (i.e., planning CTs and CBCTs) were manually contoured slice-by-slice by one radiation oncologist. These contours were the primary CTV, including the cervix, uterus, and upper-vagina, and the rectum, bladder, and bowel bag (including the sigmoid). These delineations were considered as the reference in this study.

2.2 CBCT segmentation using deep-learning

The segmentation model was trained using the deep learning-based method nnU-Net, which has been demonstrated to be efficient in multiple medical image segmentation tasks (Isensee *et al* 2021). nnU-Net's automatic configuration runs without human intervention when it is applied to a new dataset. The nnU-Net focuses on pre-processing, training, inference strategies, and post-processing. The 3D full resolution U-Net was used since it has been shown to be one of the best performing models in many medical image segmentation tasks (Malimban *et al* 2022, Isensee *et al* 2021).

All images were cropped to the region of nonzero values with a cropping size of 84×410×410 voxels. The resampling voxel size was the median voxel spacing of the dataset, i.e., 1.00×1.00×2.00 mm^3. A z-score normalization was applied to each image. In the post-processing procedure, a connected component analysis was performed to eliminate the detection of spurious false positives. The model was trained using Pytorch and stochastic gradient descent (SGD) optimizer. The initial learning rate was set to 0.01 and decreased according to the "Poly" scheme (Chen *et al* 2017). The loss function was the sum of Dice similarity coefficient and cross-entropy with the same weight.

We randomly split all 23 patients into four folds using a cross-validation scheme. Table 1 presents the partition of the dataset. Multiple images (i.e., planning and daily images) from individual patients were not distributed among datasets. The test data was only used to evaluate the performance of the model in this fold and was not involved in training. nnU-Net further divided the training data into training and validation sets and performed a five-fold cross-validation to automatically select the best network configuration. In the end, the model (or ensemble) which got the best performance was chosen to perform the inference on the test sets of this fold. The number of epochs during training was 1000 for every fold. The evaluation of the segmented volumes is described in part 2.4.1. Table 2 reports the network configurations generated by nnU-Net for the considered dataset.

2.3 Plan-of-the-day selection

After obtaining the segmentation results for each CBCT image, the following three steps were performed: (1) Bone-based rigid registration between each pCT with different bladder fillings (FB, IB, EB) and the daily CBCT to simulate patient repositioning; (2) computation of the coverage between the CTV of CBCT ($\boldsymbol{CTV_{CBCT}}$) and CTV of the CTs ($\boldsymbol{CTV_{EB}}, \boldsymbol{CTV_{IB}}, \boldsymbol{CTV_{FB}}$); (3) selection of the pCT corresponding to the best coverage.

Model	#Patient		#CBCT volume	
	Train	Test	Train	Test
1	18	5	216	56
2	17	6	197	75
3	17	6	206	66
4	17	6	199	73

Table 1. Partition of the dataset for the deep learning network training and testing. The population was randomly separated into four folds using a cross-validation scheme to evaluate the model performance. Multiple images (i.e., planning and daily images) from individual patients were not distributed among datasets.

Parameters	3D full resolution U-Net
Normalization	Z normalization
Patch size	$56 \times 192 \times 160$
Batch size	2
Downsampling strides	[[1, 2, 2], [2, 2, 2], [2, 2, 2], [2, 2, 2], [1, 2, 2]]
Convolution kernel sizes	[[1, 3, 3], [3, 3, 3], [3, 3, 3], [3, 3, 3], [3, 3, 3], [3, 3, 3]]

Table 2. Network configurations generated by nnU-Net.

2.3.1 Rigid registration

For each patient, a bone-based rigid registration was performed between each CBCT and each pCT, using the ROI of the CBCT which was limited to the treated region. The goal of rigid registration was, in this study, to simulate patient repositioning. In the clinical setup, the rigid transform would result from the applied couch shift/rotation. The library Elastix was used *(Klein* et al *2009)* to estimate the rigid transform (translation and rotation) with normalized correlation as the metric, applied to thresholded images. The resulting rigid transform was visually validated by checking bone alignment and was applied to the pCT's corresponding delineations.

2.3.2 Selection of the PoD

To evaluate the ability of each treatment plan to treat the CTV in its daily position, a coverage index was computed between the $\boldsymbol{CTV_{CBCT}}$ segmented by the deep learning model and the different CTV of the patients's library ($\boldsymbol{CTV_{CT}} \in \{\boldsymbol{CTV_{EB}}, \boldsymbol{CTV_{IB}}, \boldsymbol{CTV_{FB}}\}$)*:*

$$\boldsymbol{cov} = \frac{|\boldsymbol{CTV_{CBCT}} \cap \boldsymbol{CTV_{CT}}|}{|\boldsymbol{CTV_{CT}}|} \quad (1)$$

where | . | is the cardinality of the set. In this way, each CBCT had a coverage value associated with each of the three pCTs (IB, EB, FB) of the patient.

All the three pCTs of the considered patient were ranked according to the corresponding coverage. The pCT corresponding to the highest coverage value was selected as the PoD of the considered treatment fraction.

2.4 Evaluation

The data of the 23 patients were used to evaluate the proposed PoD selection process.

2.4.1 Segmentation evaluation

The segmentation of CBCT images was evaluated using four-fold cross-validation, considering the manual expert delineations as the reference. The following geometric metrics were computed for CTV, bowel bag, rectum, and bladder.

i) Volume-based metric

The Dice similarity coefficient (DSC) allows for comparing the automatic segmentation results (Sp) with the reference delineation (Sr) where a perfect overlap returns 1, and no overlap returns 0:

$$DSC = 2\frac{|S_r \cap S_p|}{|S_r| + |S_p|} \quad (2)$$

ii) Distance-based metrics

Distance-based metrics allow for evaluating the segmentation in terms of the location and shape accuracies of the segmented region boundaries. They use two point sets, A and B, from Sp and Sr. N is the number of points in A.

Mean absolute distance (MAD) measures the average distance of one boundary pixel to the closest boundary pixels in the other segmentation:

$$MAD = \frac{1}{N}\sum_{a \in A} \min_{b \in B} \|a - b\| \quad (3)$$

Hausdorff distance (HD) measures the similarity between two boundaries and can be expressed as:

$$HD = max\,(h(A,B),h(B,A)) \quad (4)$$

where $h(A,B) = \max_{a \in A} \min_{b \in B} \|a - b\|$. We reported HD95, i.e., the 95th percentile of HD, to limit the influence of small outliers.

2.4.2 PoD selection evaluation

For each treatment fraction, the PoD resulting from the proposed automatic process was compared to the one obtained using the reference delineation of the CTV in the CBCT image. Thus, this reference PoD corresponded to the best coverage between the manual delineation of the $\boldsymbol{CTV_{CBCT}}$ and $\boldsymbol{CTV_{CT}} \in \{\boldsymbol{CTV_{EB}}, \boldsymbol{CTV_{IB}}, \boldsymbol{CTV_{FB}}\}$.

To consider that multiple treatment plans may provide a satisfying coverage of the target, a 5% tolerance was applied to the maximum coverage, and the corresponding treatment plan(s) were also selected.

The accuracy of the PoD selection was determined by calculating the number of automatically selected PoD that were identical to the reference PoD or included in the selected treatment plans.

3. Results

3.1 Performance of segmentation

Table 3 reports the mean (range) values of the geometric metrics for the automatic segmentation**.** Figure 3 summarizes the quantitative results in boxplots. The median DSC of primary CTV, bowel bag, rectum, and bladder were 0.79, 0.81, 0.75, and 0.84, respectively. Figure 4 shows the results of automatic contouring for four patients in axial and sagittal views.

Organ	DSC	MAD (mm)	HD95 (mm)
CTV	0.79 (0.42 - 0.94)	2.90 (0.65 - 11.48)	10.49 (3.02 - 46.43)
Bowel bag	0.81 (0.53 - 0.92)	5.22 (2.12 - 12.15)	18.40 (6.12 - 60.43)
Rectum	0.75 (0.30 - 0.91)	3.14 (0.65 - 16.04)	14.19 (2.24 - 78.79)
Bladder	0.84 (0.13 - 0.96)	2.91 (0.61 - 17.9)	9.45 (2.03 - 58.22)

Table 3. Quantitative evaluation results of CBCT segmentation.

DSC = Dice similarity coefficient ; MAD = Mean absolute distance ; HD95 = 95 th percentile Hausdorff Distance

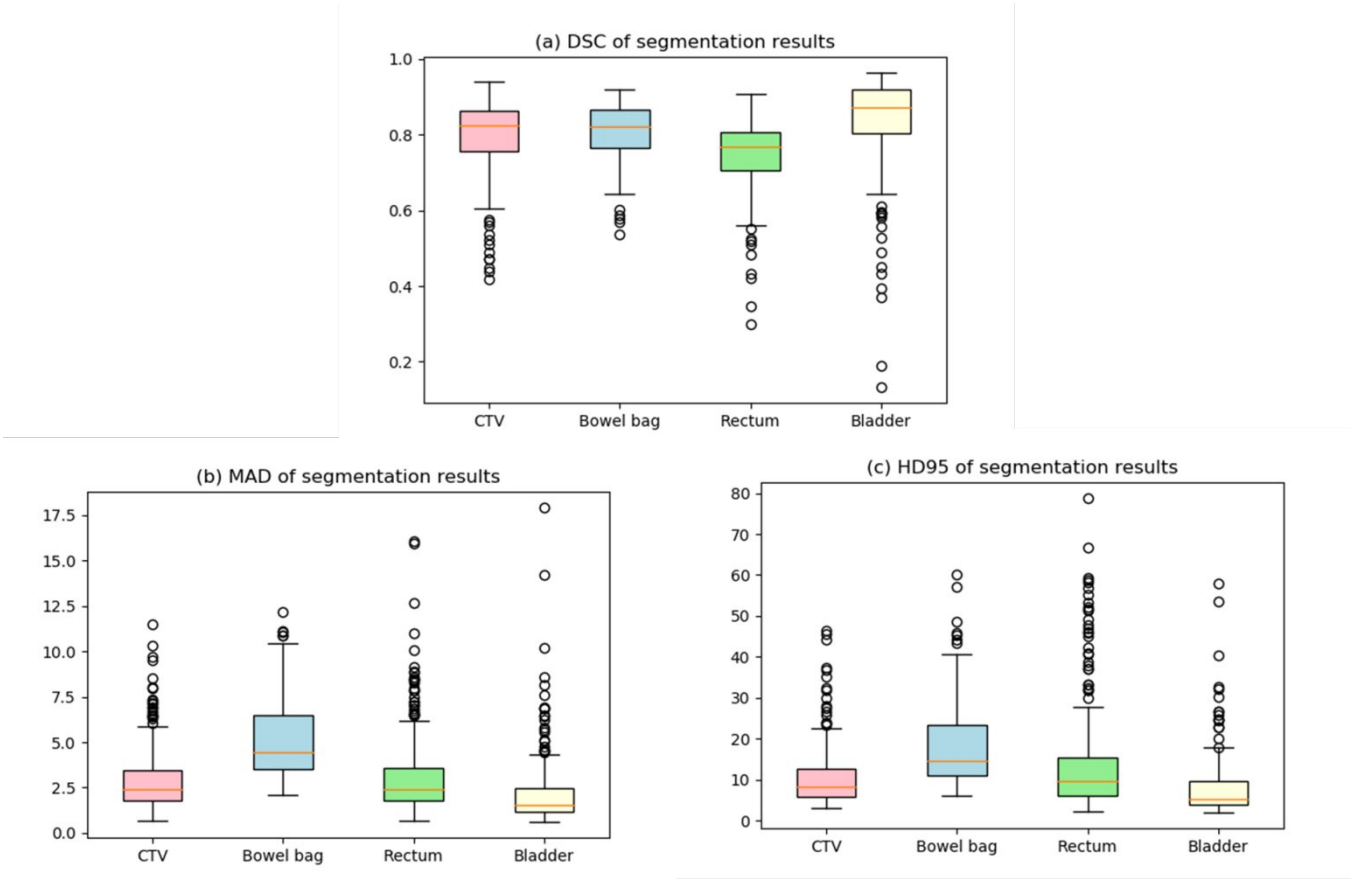

Figure 3. Quantative segmention results of CTV (uterus), bowel bag, rectum and bladder presented as boxplots. (a) DSC = Dice similarity coefficient ; (b) MAD = Mean absolute distance ; (c) HD95 = 95th percentile Hausdorff Distance

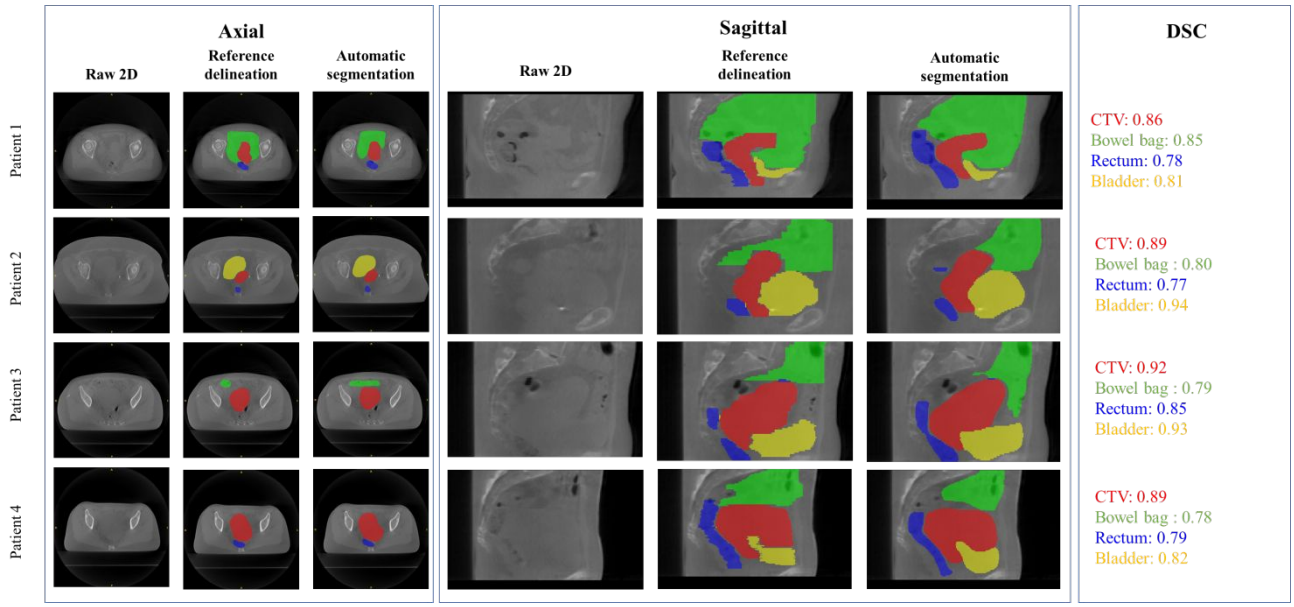

Figure 4. Examples of segmentation on CBCT. The contours are represented on the axial and sagittal views in red, green, yellow and blue for the primary CTV, bowel bag, bladder and rectum, respectively. DSC: Dice similarity coefficient.

3.1 Performance of treatment plan selections

Considering the accuracy of automatic PoD selection without the 5% tolerance, an agreement between the reference PoD and the automatically identified PoD was observed for 91.5% of CBCTs. This resulted in 23 out of 272 tested CBCTs having a suboptimal selected PoD, compared to the reference.

Using the 5% tolerance value for PoD selection, multiple (up to three) pCTs could be selected as optimal PoD. This resulted in

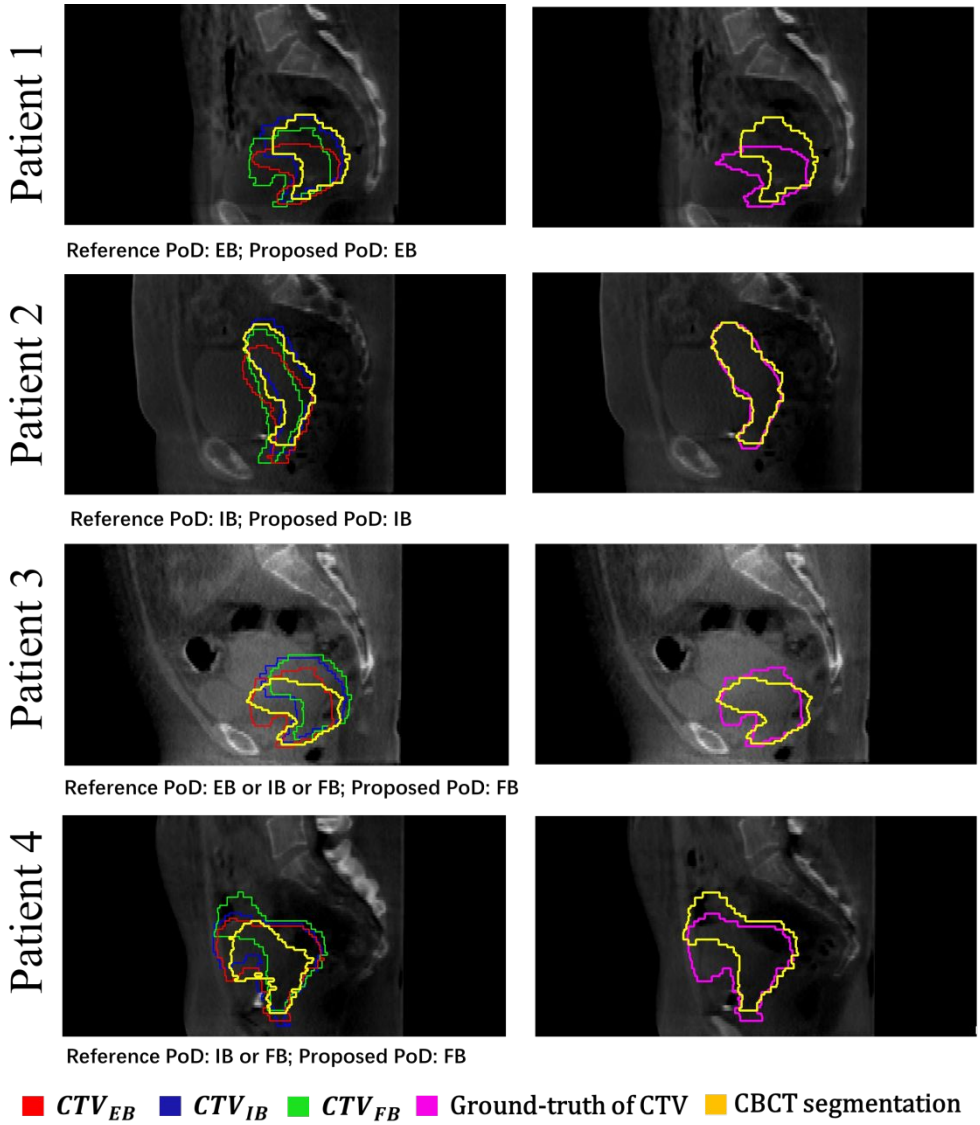

Figure 5. Examples of automatic PoD selection for four patients. (Left) Result of segmentation and clinical target volumes (CTVs) corresponding to the planning library for PoD selection; (Right) Automatic and reference CTV segmentations. Illustrated patients were selected based on the following criteria: single selected PoD (Patients 1 and 2); multiple PoD selections due to the tolerance value of 5% (Patient 3 and 4).

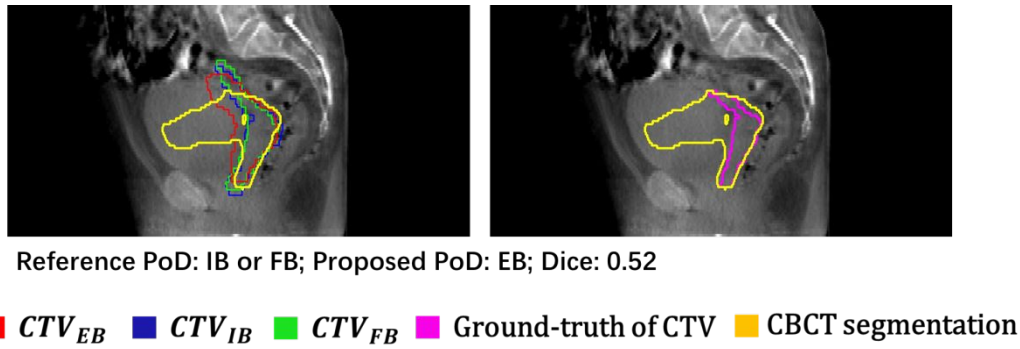

Figure 6. One case with suboptimal PoD selection. (Left) Result of segmentation and clinical target volumes (CTVs) corresponding to the planning library for PoD selection; (Right) Automatic and reference CTV segmentations. The poor segmentation of CTV results in the suboptimal PoD selection.

an increased PoD selection agreement to 99.6%, with one CBCT having suboptimal PoD selection. Figure 5 shows the PoD selection on four different patients corresponding to an agreement between the proposed and selected PoDs. Figure 6 illustrates the only case with suboptimal PoD selection. For this case, the automatic segmentation results were poor (Dice of CTV segmentation was 0.52), which resulted in the wrong proposed PoD.

4. Discussion

This study aimed at improving the PoD selection for LACC ART on CBCT images. Simulating the proposed process on 272 treatment fractions, it resulted in an agreement between the reference PoD and the automatically identified PoD for all fractions except one.

The first step of the process was based on the automatic segmentation of the daily images using a deep learning network. The resulting average DSC on the 272 CBCT images were higher than 0.75 for the primary CTV and the three main OARs (bowel bag, rectum, and bladder).

Only two works in the literature, to the best of our knowledge, have proposed cervix CBCT automatic segmentation (Langerak *et al* 2014, Beekman *et al* 2022). Langerak et al. (Langerak *et al* 2014) used a multi-atlas-based segmentation method. On a total of 224 CBCT, the images corresponding to low confidence levels were firstly removed, resulting to 187 images on which the Dice values were 0.85, 0.81, and 0.80 for the uterus, bladder, and rectum, respectively. Without discarding any CBCT image, the DSC values obtained in our study were close to these ones, with lower values for CTV and rectum, and higher values for bladder. More recently, Beekman et al. (Beekman *et al* 2022) compared different deep learning approaches and showed that the best performances were obtained by a deformation-based registration network with a mean DSC of 0.80 on the uterus, computed on a test set of 20 CBCT images. In our study, we obtained similar DSC on 272 CBCT images. This study and (Beekman *et al* 2022) are the only ones using deep learning for cervix CBCT segmentation. Although 2D and 3D U-Net (or V-Net) networks have been used on planning CT images (Liu *et al* 2020, Rhee *et al* 2020, Rigaud *et al* 2021) resulting to larger DSC for CTV (0.86 ± 0.08), lower contrast, higher noise, but also limited availability of reference segmentation, challenge the exploitation of these methods on CBCT. To our knowledge, this is the first study exploiting nnU-Net on CBCT images and on the uterine region. It confirms its good performances which have been shown on other imaging modalities (Isensee *et al* 2021).

In this study, the deep learning model was trained to segment not only the CTV (which is important for PoD selection), but also the main OARs. Intuitively, a binary segmentation task (segmenting only CTVs) could be easier than a multi-class segmentation task (segmenting OARs and CTVs) and thus could achieve better segmentation results. However, in terms of geometric considerations, multi-class segmentation provides a positional prior (e.g. the uterus should be between the bladder and rectum). Such a positional prior helps the convolutional neural network to constrain the position of the uterus during segmentation. Preliminary experiments have validated this assumption, with better results when including OARs in the segmentation task.

The evaluation of the proposed process, not only in terms of segmentation accuracy (e.g., with Dice score) but in terms of PoD selection, is of clinical interest since this PoD selection is, in this adaptive strategy, the most important and difficult step.

In the current clinical practice, the treatment plan is selected visually, resulting in potentially high inter-observer variations (Gobeli *et al* 2018). The identification of the optimal treatment plan appears particularly difficult in the context of complex deformations and limited image quality. Langerak et al. (Langerak *et al* 2014) proposed a PoD selection, after CBCT segmentation, by comparing the segmented bladder volume to the preoperative planning library (empty and full bladder). However, the CTV shape may be influenced by other factors than bladder filling, including rectum filling, tumor shrinkage, or non-moving cervix. The PoD selection should thus ideally be primarily based on the shape of the target.

In this paper, the criteria used to select the PoD was the coverage of the daily CTV by the CTVs corresponding to the different planning CTs. It enabled to consider directly the treatment of the target instead of a surrogate of the target position. Moreover, selecting the best plan as the one providing the best CTV coverage is the approach considered in the literature (Gobeli *et al* 2018, Heijkoop *et al* 2014). On the other hand, since the OARs were also segmented in the proposed process, considering the OARs in the PoD selection is technically possible. However, it would require the definition of a decision process, or a metric, considering and weighting the different criteria (CTV and OARs coverage).

In our study, only 1 case (out of 272) resulted in wrong PoD selection (Figure 6). This case with a relatively small uterus, was caused by poor segmentation result. In a clinical context, this kind of result would be easily visually detected. Then, the treatment plan could be manually selected in the library or a backup plan could be used as proposed in (Heijkoop *et al* 2014).

Online adaptive radiotherapy has recently seen important improvements, especially with the development of MRI-linac and CBCT-based online optimization. For both of them, some challenges remain and hamper their clinical deployment to treat cervical cancer, including the limited quality of CBCT images and long treatment times of MRI-Linac. Very few studies have thus considered these kinds of systems to treat cervical cancer patients (Shelley *et al* 2021, Yock *et al* 2021). Moreover, the combination of online adaptation with PoD strategies may be of interest to optimize the clinical workflow and limit treatment times.

There are some limitations to our study. The PoD selection criterion was only based on geometrical coverage. It may be of interest to consider dosimetric criteria, which is challenging since it would require computing the dose distribution on the CBCT images. Another limitation is related to the limited number of patients in this study. The proposed workflow will have to be evaluated on a larger cohort. Especially, the evaluation of the segmentation network will have to be deepened, potentially resulting in the need to improve the robustness of the model by training it with new data. Finally, the PoD ART strategy based on multiple planning CTs has shown some limitations, and some more complex strategies have been proposed to improve the libraries. For example, an “evolutive library” strategy has been proposed, enriching the library by including some CBCT anatomies into the library when the daily clinical target volume (CTV) shape differed from the ones in the library (Rigaud *et al* 2018). Including modeled anatomies resulting from a population analysis has also been proposed (Rigaud *et al* 2019). All

these strategies are based on daily PoD selection, and thus combining the proposed PoD selection method with them should be investigated.

5. Conclusion

This work proposed and evaluated an automatic workflow to select PoD for LACC ART. Based on CBCT image segmentation using a deep-learning method, it selects the optimal treatment plan based on daily CTV geometrical coverage. The evaluation of 272 treatment fractions showed a high agreement with the reference resulting from expert delineation. The proposed workflow should be further evaluated in a clinical workflow and on a larger number of patients.

Acknowledgments

This work was partly funded by the French National Research Association (ANR) as part of the Investissement d'Avenir programme (Labex CAMI) under reference ANR- 11-LABX-0004, by the DELPEL project with financial support from ITMO Cancer AVIESAN (National Alliance for Life Sciences & Health) within the framework of the Cancer Plan, by the French organizations "Ligue contre le Cancer" and "La Vannetaise", and by the Embassy of France in China.

Ethical Statement

This research was conducted in accordance with the principles embodied in the Declaration of Helsinki and in accordance with local statutory requirements. It has been approved by the regional research ethics committee (Comité de Protection des Personnes, Ouest V, Rennes, AR-COL 2015-02-45-01). All participants gave written informed consent to participate in the study.

References

Beadle B M, Jhingran A, Salehpour M, Sam M, Iyer R B and Eifel P J 2009 Cervix regression and motion during the course of external beam chemoradiation for cervical cancer *International Journal of Radiation Oncology* Biology* Physics* **73** 235–41

Beekman C, van Beek S, Stam J, Sonke J-J and Remeijer P 2022 Improving predictive CTV segmentation on CT and CBCT for cervical cancer by diffeomorphic registration of a prior *Medical physics* **49** 1701–11

Bondar M L, Hoogeman M S, Mens J W, Quint S, Ahmad R, Dhawtal G and Heijmen B J 2012 Individualized nonadaptive and online-adaptive intensity-modulated radiotherapy treatment strategies for cervical cancer patients based on pretreatment acquired variable bladder filling computed tomography scans *International Journal of Radiation Oncology* Biology* Physics* **83** 1617–23

Bondar M L, Hoogeman M, Schillemans W and Heijmen B 2013 Intra-patient semi-automated segmentation of the cervix–uterus in CT-images for adaptive radiotherapy of cervical cancer *Physics in Medicine & Biology* **58** 5317

Buchali A, Koswig S, Dinges S, Rosenthal P, Salk J, Lackner G, BoÈhmer D, Schlenger L and Budach V 1999 Impact of the filling status of the bladder and rectum on their integral dose distribution and the movement of the uterus in the treatment planning of gynaecological cancer *Radiotherapy and oncology* **52** 29–34

Chan P, Dinniwell R, Haider M A, Cho Y-B, Jaffray D, Lockwood G, Levin W, Manchul L, Fyles A and Milosevic M 2008 Inter-and intrafractional tumor and organ movement in patients with cervical cancer

undergoing radiotherapy: a cinematic-MRI point-of-interest study *International Journal of Radiation Oncology* Biology* Physics* **70** 1507–15

Chen L-C, Papandreou G, Kokkinos I, Murphy K and Yuille A L 2017 Deeplab: Semantic image segmentation with deep convolutional nets, atrous convolution, and fully connected crfs *IEEE transactions on pattern analysis and machine intelligence* **40** 834–48

Ding S, Liu H, Li Y, Wang B, Li R, Liu B, Ouyang Y, Wu D and Huang X 2021 Assessment of dose accuracy for online MR-guided radiotherapy for cervical carcinoma *Journal of Radiation Research and Applied Sciences* **14** 159–70

Gandhi A K, Sharma D N, Rath G K, Julka P K, Subramani V, Sharma S, Manigandan D, Laviraj M A, Kumar S and Thulkar S 2013 Early clinical outcomes and toxicity of intensity modulated versus conventional pelvic radiation therapy for locally advanced cervix carcinoma: a prospective randomized study *International Journal of Radiation Oncology* Biology* Physics* **87** 542–8

Gobeli M, Rigaud B, Charra-Brunaud C, Renard S, De Rauglaudre G, Beneyton V, Racadot S, Peignaux K, Leseur J and Williaume D 2018 CBCT guided adaptive radiotherapy for cervix cancer: uncertainty of the choice of the plan of the day *Radiother Oncol* **127** S606–7

Gobeli M, Simon A, Getain M, Leseur J, Lahlou E, Lafond C, Dardelet E, Williaume D, Rigaud B and de Crevoisier R 2015 Benefit of a pretreatment planning library-based adaptive radiotherapy for cervix carcinoma? *Cancer Radiotherapie: Journal de la Societe Francaise de Radiotherapie Oncologique* **19** 471–8

Han Y, Shin E H, Huh S J, Lee J E and Park W 2006 Interfractional dose variation during intensity-modulated radiation therapy for cervical cancer assessed by weekly CT evaluation *International Journal of Radiation Oncology* Biology* Physics* **65** 617–23

Heijkoop S T, Langerak T R, Quint S, Bondar L, Mens J W M, Heijmen B J and Hoogeman M S 2014 Clinical implementation of an online adaptive plan-of-the-day protocol for nonrigid motion management in locally advanced cervical cancer IMRT *International Journal of Radiation Oncology* Biology* Physics* **90** 673–9

Isensee F, Jaeger P F, Kohl S A, Petersen J and Maier-Hein K H 2021 nnU-Net: a self-configuring method for deep learning-based biomedical image segmentation *Nature methods* **18** 203–11

Jadon R, Pembroke C A, Hanna C L, Palaniappan N, Evans M, Cleves A E and Staffurth J 2014 A systematic review of organ motion and image-guided strategies in external beam radiotherapy for cervical cancer *Clinical oncology* **26** 185–96

Klein S, Staring M, Murphy K, Viergever M A and Pluim J P 2009 Elastix: a toolbox for intensity-based medical image registration *IEEE transactions on medical imaging* **29** 196–205

Langerak T, Heijkoop S, Quint S, Mens J-W, Heijmen B and Hoogeman M 2014 Towards automatic plan selection for radiotherapy of cervical cancer by fast automatic segmentation of cone beam CT scans *International Conference on Medical Image Computing and Computer-Assisted Intervention* (Springer) pp 528–35

Liu Z, Liu X, Xiao B, Wang S, Miao Z, Sun Y and Zhang F 2020 Segmentation of organs-at-risk in cervical cancer CT images with a convolutional neural network *Physica Medica* **69** 184–91

Malimban J, Lathouwers D, Qian H, Verhaegen F, Wiedemann J, Brandenburg S and Staring M 2022 Deep learning-based segmentation of the thorax in mouse micro-CT scans *Sci Rep* **12** 1822

Naik A, Gurjar O P, Gupta K L, Singh K, Nag P and Bhandari V 2016 Comparison of dosimetric parameters and acute toxicity of intensity-modulated and three-dimensional radiotherapy in patients with cervix carcinoma: A randomized prospective study *Cancer Radiother* **20** 370–6

Rhee D J, Jhingran A, Rigaud B, Netherton T, Cardenas C E, Zhang L, Vedam S, Kry S, Brock K K and Shaw W 2020 Automatic contouring system for cervical cancer using convolutional neural networks *Medical physics* **47** 5648–58

Rigaud B, Anderson B M, Zhiqian H Y, Gobeli M, Cazoulat G, Söderberg J, Samuelsson E, Lidberg D, Ward C and Taku N 2021 Automatic segmentation using deep learning to enable online dose optimization during adaptive radiation therapy of cervical cancer *International Journal of Radiation Oncology* Biology* Physics* **109** 1096–110

Rigaud B, Simon A, Gobeli M, Lafond C, Leseur J, Barateau A, Jaksic N, Castelli J, Williaume D and Haigron P 2018 CBCT-guided evolutive library for cervical adaptive IMRT *Medical physics* **45** 1379–90

Rigaud B, Simon A, Gobeli M, Leseur J, Duverge L, Williaume D, Castelli J, Lafond C, Acosta O, Haigron P and De Crevoisier R 2019 Statistical Shape Model to Generate a Planning Library for Cervical Adaptive Radiotherapy *IEEE Trans Med Imaging* **38** 406–16

van de Schoot A J, de Boer P, Visser J, Stalpers L J, Rasch C R and Bel A 2017 Dosimetric advantages of a clinical daily adaptive plan selection strategy compared with a non-adaptive strategy in cervical cancer radiation therapy *Acta oncologica* **56** 667–74

Shelley C E, Barraclough L H, Nelder C L, Otter S J and Stewart A J 2021 Adaptive Radiotherapy in the Management of Cervical Cancer: Review of Strategies and Clinical Implementation *Clinical Oncology* **33** 579–90

Yock A D, Ahmed M, Ayala-Peacock D, Chakravarthy A B and Price M 2021 Initial analysis of the dosimetric benefit and clinical resource cost of CBCT-based online adaptive radiotherapy for patients with cancers of the cervix or rectum *J Appl Clin Med Phys* **22** 210–21